

# Spatial Resolution and Contrast Enhancement in Photoacoustic Imaging with Filter Delay Multiply and Sum Beamforming Technique

Abdulrhman Alshaya, Sevan Harput, Asraf M. Moubark, David M. J. Cowell, James McLaughlan, and Steven Freear  
Ultrasound Group, School of Electronic and Electrical Engineering, University of Leeds, UK.  
E-mail: ml11a7a@leeds.ac.uk and S.Freear@leeds.ac.uk

**Abstract**—Photoacoustic imaging is used to differentiate between tissue types based on light absorption. Different structures, such as vascular density of capillaries in human tissue, can be analysed and provide diagnostic information to detect early stage breast cancer. Delay and sum (DAS) beamforming is the traditional method to reconstruct photoacoustic images. However, for structures located deep in the tissue (>10 mm), signal to noise (SNR) of the photoacoustic signal drops significantly. This study proposes using filter delay multiply and sum (FDMAS) beamforming technique to increase the SNR and enhance the image quality. Experimental results showed that FDMAS beamformer improved the SNR by 6.9 dB and the lateral resolution by 48% compared to the DAS beamformer. Moreover, the effect of aperture size on the proposed method is presented as the sub-group FDMAS, which further increased the improvement in image quality.

## I. INTRODUCTION

Photoacoustic imaging is a type of medical imaging that combines ultrasound resolution and optical contrast. This type of imaging is created by applying short laser pulse on biological tissues [1]. Endogenous chromophores such as oxy-haemoglobin and deoxy-haemoglobin will absorb a certain wavelength laser pulse [1]. This leads to an increase in temperature at the region of interest and generation of ultrasound waves [1]. These ultrasound waves are generated due to thermoelastic expansion of the absorbent, which will be detected by using a medical ultrasound transducer. The acquired information will be used to reconstruction photoacoustic images by using one of photoacoustic beamforming technique such as time reversal, Fourier transform and delay and sum (DAS) beamforming techniques [1]–[4].

Photoacoustic imaging is used to differentiate between tissue types based on light absorption. Different structures, such as vascular density of capillaries in human tissue, can be analysed and provide diagnostic information to detect early stage breast cancer. However, signal to noise ratio (SNR) of photoacoustic image will drop when the penetration depth of the target object is increased or the optical energy of laser pulse is reduced. This is due to absorption and scattering of laser light in the biological tissue before reaching the target object. In addition, the generated acoustic signals due to photoacoustic effect will be attenuated before received by

an ultrasound transducer. Moreover, speed of ultrasound is assumed to be constant inside the biological tissue during the beamforming operation. As a result, quality of photoacoustic image will be degraded due to phase aberrations. Park *et al.* tried to deal with this issue by using adaptive beamforming technique, such as implementation of the coherence factor [5], [6].

In this study, filter delay multiply and sum (FDMAS) beamforming technique is proposed to improve SNR and resolution of a photoacoustic image. The FDMAS beamforming technique depends on autocorrelation between the RF data received by individual elements of the ultrasound probe [7]. The idea of this beamforming technique is taken from Delay multiply and sum (DMAS) beamforming technique that is applied on radar microwave to detect early stage of breast cancer [8]. In addition, this technique shows improvement in image resolution when it is applied on ultrasound imaging [7].

The proposed method used to construct photoacoustic images for 3 static scatterers embedded in an ultrasound phantom with ultrasound system and a pulse laser diode (PLD). These photoacoustic images will be constructed by using FDMAS and DAS beamforming techniques. These images will be compared in terms of SNR and spatial resolution.

## II. THEORETICAL ANALYSIS FOR FDMAS BEAMFORMING

FDMAS beamforming technique depends on autocorrelation between delayed RF data. This autocorrelation operation will improve SNR by reducing the uncorrelated signal (Noise) as shown in Eq.(1) [7]:

$$y_{FDMAS} = \left\{ \sum_{i=1}^{N-1} \sum_{j=i+1}^N \text{sign}(S_i(t)S_j(t)) \cdot \sqrt{|S_i(t)S_j(t)|} \right\} * f \quad (1)$$

where  $y_{FDMAS}$  is the output of FDMAS beamforming technique,  $N$  is the number of transducer elements and  $S_i(t)S_j(t)$  are the delayed RF data signal for  $i$  element and  $j$  element respectively. In FDMAS equation, Sign operation is used to maintain a sign of the delayed RF data after the multiplication operation [7]. In addition, square root operation is applied on the multiplied delayed RF data to remove

the effect of multiplication operation on unit of delayed RF data [7]. Furthermore, bandpass filter ( $f$ ) is applied before generating the output of FDMAS beamforming technique [7]. This is because the multiplication operation between signals in FDMAS beamforming technique generates two frequency bands. One of them is the result of summing frequency bands of multiplied signals while the other is the result of subtracting frequency bands of multiplied signals. Therefore, the bandpass filter is used to extract the high frequency band of generated signal.

In the FDMAS beamforming technique, all delayed RF data will be correlated with each other and summed. This could be drawback, if the generating photoacoustic signal is not received by all elements of the linear ultrasound transducer. For instance, if the place of the absorbent is in the corner of the linear transducer. This is because the generated photoacoustic signals will be correlated with noise signal that results in reducing the SNR of photoacoustic image. To deal with this problem, sub-group of delayed RF data signals will be correlated with each other rather than correlated all of them as shown in Eq.(2):

$$y_{FDMAS} = \left\{ \sum_{i=1}^N \sum_{j=i+1}^m \text{sign}(S_i(t)S_j(t)) \cdot \sqrt{|S_i(t)S_j(t)|} \right\} * f \quad (2)$$

where:

$$m = \begin{cases} i+s, s < N-i \\ N, \text{else} \end{cases}$$

$s$  is a group size of delayed RF data. This size will be selected based on the position of the light absorbent from the linear transducer. For example, when the light absorbent is closed to the linear transducer, the group size of the correlation operation will be small. This is because the number of transducer elements that receive the photoacoustic signal will be reduced when a target become close to the transducer. Whereas, the group size will be increased when the distances between the light absorbent and transducer is increased.

### III. EXPERIMENT SETUP

In this experiment, measurements were performed on a polyacrylamide hydrogel phantom with carbon fibre rods as shown in Fig.1. The recipe of this phantom is taken from this reference [9]. However, no scattering material is used in this phantom due to weakness of optical energy of a laser source that is used in this experiment. The setup of this experiment is shown in Fig.2. The photoacoustic signals were generated from the phantom by using 905nm PLD (905D3s3J09S). The pulse width and the output optical energy from this PLD is 100 ns and 10  $\mu$ J/pulse respectively. These generated photoacoustic signals were acquired by the Leeds Ultrasound Array Research Platform II (UARP II) with a 128 element linear 3-8 MHz transducer. When the photoacoustic signals received by UARP II, these photoacoustic signals were amplified 24 dB by using a low noise amplifier (LAN). Then these signals were amplified 30 dB by using Programmable Gain Amplifier (PGA). These received photoacoustic signals were averaged 100 times. After

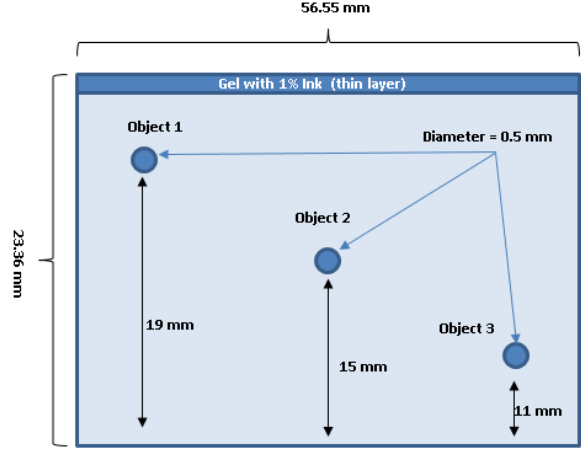


Fig. 1. The polyacrylamide hydrogel phantom with carbon fibre rods.

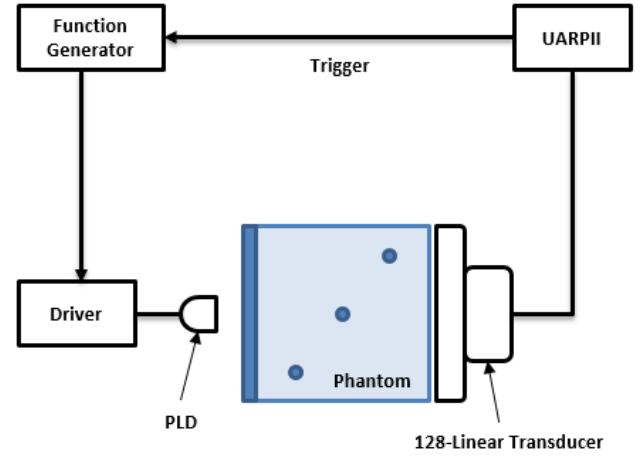


Fig. 2. The experiment setup for generating photoacoustic signals from carbon fibre rods by using PLD.

that, these received data were processed by using DAS and FDMAS beamforming techniques.

### IV. RESULT AND DISCUSSION

Fig.3 shows photoacoustic images for object 2 by using DAS and FDMAS beamforming techniques. From this figure it can be noticed that FDMAS achieved improvement over DAS in terms of SNR by 6.9 dB. This is because the effect of phase aberrations and noise signals were reduced due to the correlation operation that FDMAS used. This improvement in SNR will be almost 12 dB, if a photoacoustic signal that travels to laser source is used in image reconstruction. This is because object part that near to laser source will absorbed more optical energy. The point spread function of a single scatterer located at 15 mm depth allowed the axial and lateral resolutions to be compared as shown in Fig.4 (A) and (B) respectively. The full width at half maximum (FWHM) axial resolution was comparable in both cases, where FDMAS performing

5% better than DAS. However the FWHM resolution in the lateral direction were improved by 48%. Furthermore, by using FDMAS the side lobes were reduced especially in lateral direction.

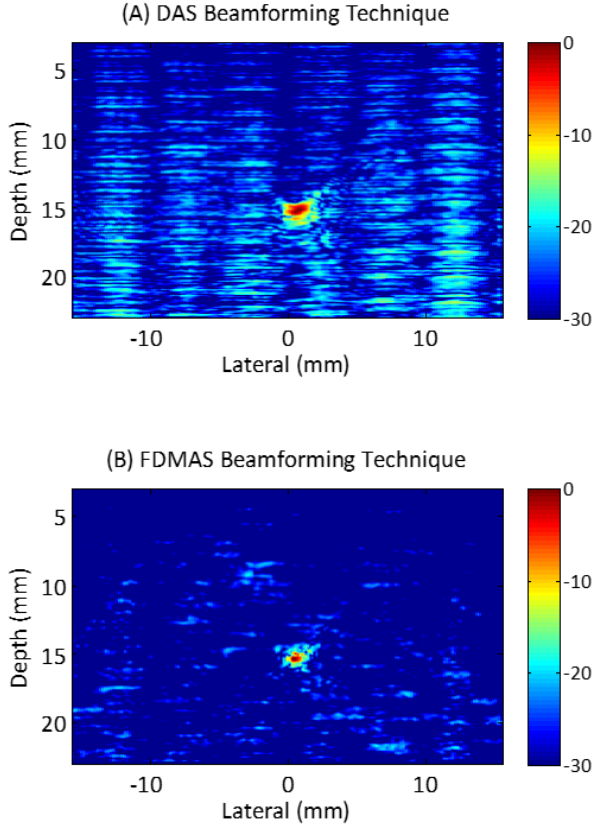


Fig. 3. (A) Photoacoustic image by using DAS and (B) Photoacoustic image by using FDMAS (30 dB dynamic range).

However, the improvement in image equality that FDMAS achieved is effected by the group size of correlated delayed RF data as shown in Fig.5. From this figure, it can be seen that the highest gain for object 3 when the group size of correlated delayed RF data is 16. This is because that the place of the absorbent object is in the corner of the linear transducer and close to it. As a result, not all the transducer elements will receive photoacoustic signals. Therefore, the image equality will be better when the group size becomes close to a number of elements that received acoustic signals to reduce the effect of unwanted signals. In addition, the largest gain for object 1 and object 2 when the group size of correlated delayed RF data is 32. This is because that the linear transducer has large field of view for object 1 and object 2. This is unlike the object 3. Furthermore, the optical energy that reach the object 3 is lower than the optical energy that reach object 1 and object 2. This is because the place of the laser source and ultrasound transducer in this experiment

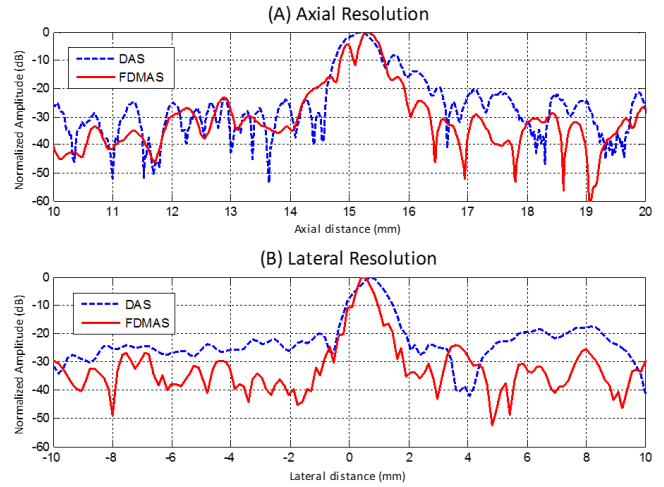


Fig. 4. (A) Axial resolution by using DAS (Blue line) and FDMAS (Red line) (B) Lateral resolution by using DAS (Blue line) and FDMAS (Red line).

which are opposite each other. Therefore, the object that close to the transducer received optical energy less compare with the object that far from transducer.

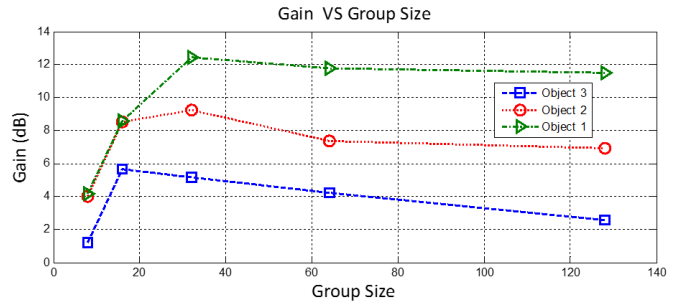


Fig. 5. The SNR gain achieved by the FDMAS for three different objects is plotted against group size.

Three sub-wavelength objects at different depths were imaged by using UARPII and processed with DAS, FDMAS and 32-FDMAS methods as shown in Fig.6. From this figure, it can be noticed that the improvement in the SNR of the photoacoustic image by using 32-FDMAS is higher than the improvement in the SNR of the photoacoustic image by using FDMAS. In addition, the processing time for 32-FDMAS is less than the processing time for FDMAS. This is because that the number of correlation operation of 32-FDMAS is less than the number of correlation operation of FDMAS.

## V. CONCLUSION

In this study, the time delay estimation of image reconstruction is improved by using FDMAS beamforming technique. In addition, FDMAS shows improvement in SNR by 6.9 dB over DAS. From point spread function of single scattering point, the FWHM axial and lateral resolution is better by 5% and 48% respectively when FDMAS is used. In this paper,

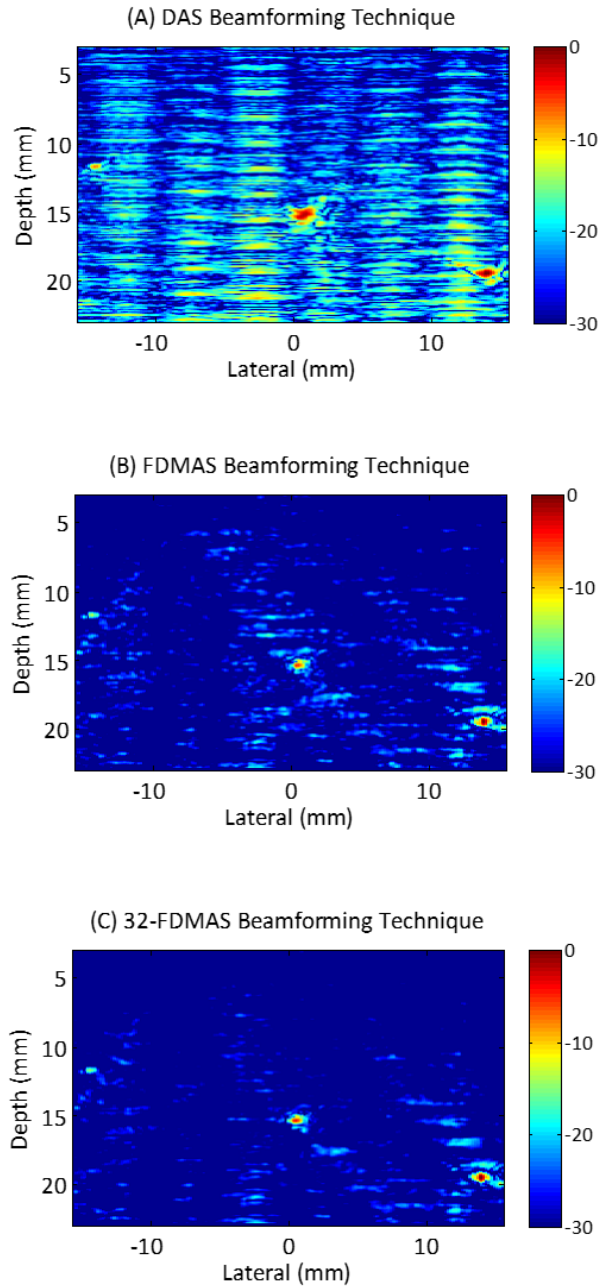


Fig. 6. (A) Photoacoustic image by using DAS, (B) Photoacoustic image by using FDMAS and (c) Photoacoustic image by using 32-FDMAS (30 dB dynamic range).

sub-group FDMAS is explained. This sub-group FDMAS shows improvement in image equality over FDAMS and DAS. However, this improvement in image quality depends on the group size of correlation points. This group size should be reduced when target object become close to linear transducer. In future work, to get the highest gain, the group size of correlation points will be dynamically changed based on image parts.

#### REFERENCES

- [1] B. E. Treeby, E. Z. Zhang, and B. Cox, "Photoacoustic tomography in absorbing acoustic media using time reversal," *Inverse Problems*, vol. 26, no. 11, p. 115003, 2010.
- [2] B. T. Cox and B. E. Treeby, "Artifact trapping during time reversal photoacoustic imaging for acoustically heterogeneous media," *IEEE transactions on medical imaging*, vol. 29, no. 2, pp. 387–396, 2010.
- [3] P. Kornel, M. Frenz, H. Bebie, H. P. Weber *et al.*, "Temporal backward projection of optoacoustic pressure transients using fourier transform methods," *Physics in medicine and biology*, vol. 46, no. 7, p. 1863, 2001.
- [4] C. Yoon, J. Kang, S. Han, Y. Yoo, T.-K. Song, and J. H. Chang, "Enhancement of photoacoustic image quality by sound speed correction: ex vivo evaluation," *Optics express*, vol. 20, no. 3, pp. 3082–3090, 2012.
- [5] S. Park, A. B. Karpiouk, S. R. Aglyamov, and S. Y. Emelianov, "Adaptive beamforming for photoacoustic imaging using linear array transducer," in *2008 IEEE Ultrasonics Symposium*. IEEE, 2008, pp. 1088–1091.
- [6] —, "Adaptive beamforming for photoacoustic imaging," *Optics letters*, vol. 33, no. 12, pp. 1291–1293, 2008.
- [7] G. Matrone, A. S. Savoia, G. Caliano, and G. Mageses, "The delay multiply and sum beamforming algorithm in ultrasound b-mode medical imaging," *IEEE transactions on medical imaging*, vol. 34, no. 4, pp. 940–949, 2015.
- [8] H. B. Lim, N. T. T. Nhung, E.-P. Li, and N. D. Thang, "Confocal microwave imaging for breast cancer detection: Delay-multiply-and-sum image reconstruction algorithm," *IEEE Transactions on Biomedical Engineering*, vol. 55, no. 6, pp. 1697–1704, 2008.
- [9] M. J. Choi, S. R. Guntur, K. I. Lee, D. G. Paeng, and A. Coleman, "A tissue mimicking polyacrylamide hydrogel phantom for visualizing thermal lesions generated by high intensity focused ultrasound," *Ultrasound in medicine & biology*, vol. 39, no. 3, pp. 439–448, 2013.